INSTITUT DE FRANCE
Académie des sciences

Comptes Rendus

Géoscience

Sciences de la Planète

Charles Masquelet, Sylvie Leroy, Matthias Delescluse, Nicolas Chamot-Rooke, Isabelle Thinon, Anne Lemoine, Dieter Franke, Louise Watremez, Philippe Werner, Fabien Paquet, Carole Berthod, Victor Cabiativa Pico and Daniel Sauter

The East-Mayotte new volcano in the Comoros Archipelago: structure and timing of magmatic phases inferred from seismic reflection data

Published online: 9 December 2022

https://doi.org/10.5802/crgeos.154

Part of Special Issue: The Mayotte seismo-volcanic crisis of 2018-2021 in the Comoros archipelago (Mozambique channel)

Guest editors: Jérôme Van der Woerd (Institut Terre Environnement de Strabourg, UMR 7063 CNRS / Université de Strasbourg, 67084 Strasbourg, France), Vincent Famin (Laboratoire Géosciences Réunion, Université de La Réunion - IPGP, 97744 Saint-Denis, France) and Eric Humler (Professeur Université de Nantes, Laboratoire de Planétologie et Géosciences, UMR 6112, Faculté des Sciences et Techniques, Nantes Université, 44322 Nante, France)

Les Comptes Rendus. Géoscience — Sciences de la Planète *sont membres du Centre Mersenne pour l'édition scientifique ouverte*
www.centre-mersenne.org
e-ISSN : 1778-7025

Comptes Rendus
Géoscience — Sciences de la Planète
Published online: 9 December 2022
https://doi.org/10.5802/crgeos.154

The Mayotte seismo-volcanic crisis of 2018-2021 in the Comoros archipelago (Mozambique channel) / *La crise sismo-volcanique de 2018-2021 de Mayotte dans l'archipel des Comores (Canal du Mozambique)*

The East-Mayotte new volcano in the Comoros Archipelago: structure and timing of magmatic phases inferred from seismic reflection data

Le nouveau volcan de l'Est-Mayotte dans l'archipel des Comores : structure et chronologie des phases magmatiques déduites des données d'imagerie sismique

Charles Masquelet*, [a], Sylvie Leroy [a], Matthias Delescluse [b], Nicolas Chamot-Rooke [b], Isabelle Thinon [c], Anne Lemoine [c], Dieter Franke [d], Louise Watremez [e], Philippe Werner [f], Fabien Paquet [c], Carole Berthod [g], Victor Cabiativa Pico [a] and Daniel Sauter [f]

[a] Sorbonne Université, CNRS, Institut des Sciences de la Terre de Paris (ISTeP), Paris, France

[b] Laboratoire de Géologie de l'École Normale Supérieure (ENS), CNRS UMR 8538, PSL University, Paris, France

[c] Bureau de Recherches Géologiques et Minières (BRGM), Orléans, France

[d] Bundesanstalt für Geowissenschaften und Rohstoffe (BGR), Hannover, Deutschland

[e] Université de Lille, CNRS, Université Littoral Côte d'Opale, IRD, UMR 8187 – LOG – Laboratoire d'Océanologie et de Géosciences, Lille, France

[f] Institut Terre et Environnement de Strasbourg (ITES), CNRS Université de Strasbourg, Strasbourg, France

[g] Laboratoire Magma et Volcans, Aubière, France

E-mails: charles.masquelet@sorbonne-universite.fr (C. Masquelet), sylvie.leroy@sorbonne-universite.fr (S. Leroy), delescluse@geologie.ens.fr (M. Delescluse), rooke@geologie.ens.fr (N. Chamot-Rooke), I.thinon@brgm.fr (I. Thinon), A.lemoine@brgm.fr (A. Lemoine), Dieter.Franke@bgr.de (D. Franke), louise.watremez@univ-lille.fr (L. Watremez), ph.werner@orange.fr (P. Werner), F.Paquet@brgm.fr (F. Paquet), carole.berthod@uca.fr (C. Berthod), victor.cabiativa_pico@sorbonne-universite.fr (V. Cabiativa Pico), Daniel.Sauter@unistra.fr (D. Sauter)

* Corresponding author.

Abstract. A multichannel seismic reflection profile acquired during the SISMAORE cruise (2021) provides the first in-depth image of the submarine volcanic edifice, named Fani Maore, that formed 50 km east of Mayotte Island (Comoros Archipelago) in 2018–2019. This new edifice sits on a ~140 m thick sedimentary layer, which is above a major, volcanic layer up to ~1 km thick and extends over 120 km along the profile. This volcanic unit is made of several distinct seismic facies that indicate successive volcanic phases. We interpret this volcanic layer as witnessing the main phase of construction of the Mayotte Island volcanic edifice. A ~2.2–2.5 km thick sedimentary unit is present between this volcanic layer and the top of the crust. A complex magmatic feeder system is observed within this unit, composed of saucer-shape sills and seal bypass systems. The deepest tip of this volcanic layer lies below the top-Oligocene seismic horizon, indicating that the volcanism of Mayotte Island likely began around 26.5 Ma, earlier than previously assumed.

Résumé. Un profil de sismique réflexion multitrace acquis lors de la campagne océanographique SISMAORE (2021) apporte la première image en profondeur du volcan sous-marin Fani Maore, qui s'est formé à 50 km à l'est de l'île de Mayotte (archipel des Comores) en 2018–2019. Ce nouvel édifice repose sur une première couche sédimentaire d'environ 140 m d'épaisseur au-dessus d'une couche volcanique majeure épaisse de 1 km et qui s'étend sur 120 km le long du profil. Cette dernière unité volcanique est constituée de plusieurs faciès sismiques distincts qui indiquent des phases volcaniques successives. Nous interprétons cette couche volcanique comme le témoin de la phase principale de construction de l'édifice volcanique de l'île de Mayotte. Une couverture sédimentaire de ~2.2–2.5 km d'épaisseur est présente entre cette couche volcanique et le toit de la croûte. On y observe de nombreux sills en forme de soucoupe ainsi que des zones à faciès de remontées de fluides, dessinant un système d'alimentation magmatique complexe sous la principale couche volcanique. L'extrémité la plus profonde de cette couche volcanique se place en dessous de l'horizon sismique de l'Oligocène supérieur et indique que le volcanisme de l'île de Mayotte a probablement commencé vers 26.5 Ma, plus tôt que ce qui était supposé auparavant.

Keywords. Comoros Archipelago, Mayotte, Fani Maore volcano, Volcanism, Seismic reflection.

Mots-clés. Archipel des Comores, Mayotte, Volcan Fani Maoré, Volcanisme, Sismique réflexion.

Published online: 9 December 2022

1. Introduction

The East-Mayotte seismo-volcanic crisis that started in May 2018 [Cesca et al., 2020, Lemoine et al., 2020] and gave birth to a large—820 m high and 5 km in diameter—submarine volcanic edifice sitting at approximately 3500 m water depth [Feuillet et al., 2021]. Following an application submitted to the UNESCO's International Marine Chart Commission, the new volcano was named Fani Maore. The new volcano grew in the abyssal plain of the North Mozambique Channel, some 50 km east of Mayotte Island (Comoros Archipelago), at the end of a NW–SE trending volcanic ridge (Figure 1). Before May 2018, no recent eruption or notable seismic activity was reported around Mayotte [Lemoine et al., 2020]. Moreover, no recent volcanic edifice was mapped during successive bathymetric surveys in 2014 and 2016 at the position of the Fani Maore volcano [Feuillet et al., 2021]. Since May 2019, multiple scientific cruises collected geophysical and geochemical data to document this active submarine eruption, which is one of the largest ever witnessed [MAYOBS cruises; Rinnert et al., 2019]. The petrological signatures of dredged lavas integrated with geophysical data show that this large effusive eruption is fed by a deep (≥37 km) and large (≥10 km^3) pre-existing mantle reservoir and that the eruption was tectonically triggered [Berthod et al., 2021a, Lavayssière et al., 2021]. The magma transfer from mantle depth up to the seafloor is syn-eruptive [Berthod et al., 2021a]. Yet, direct information at the crustal scale is missing and both the structure and the nature of the basement below the Fani Maore volcano are unknown.

In February 2021, the SISMAORE cruise aboard R/V (Research Vessel) "Pourquoi Pas?" collected deep seismic reflection data along several profiles within the abyssal plains surrounding the volcanic islands of the Comoros Archipelago (Figure 1). This article presents an interpretation of a multichannel seismic profile (MAOR21D01) acquired across the new submarine East-Mayotte volcano. This profile reveals the submarine structure of the Fani Maore volcano as well as widespread magmatic features around, sills in particular, imaged within the ~3 km thick sedimentary cover from the seafloor down to the top of the

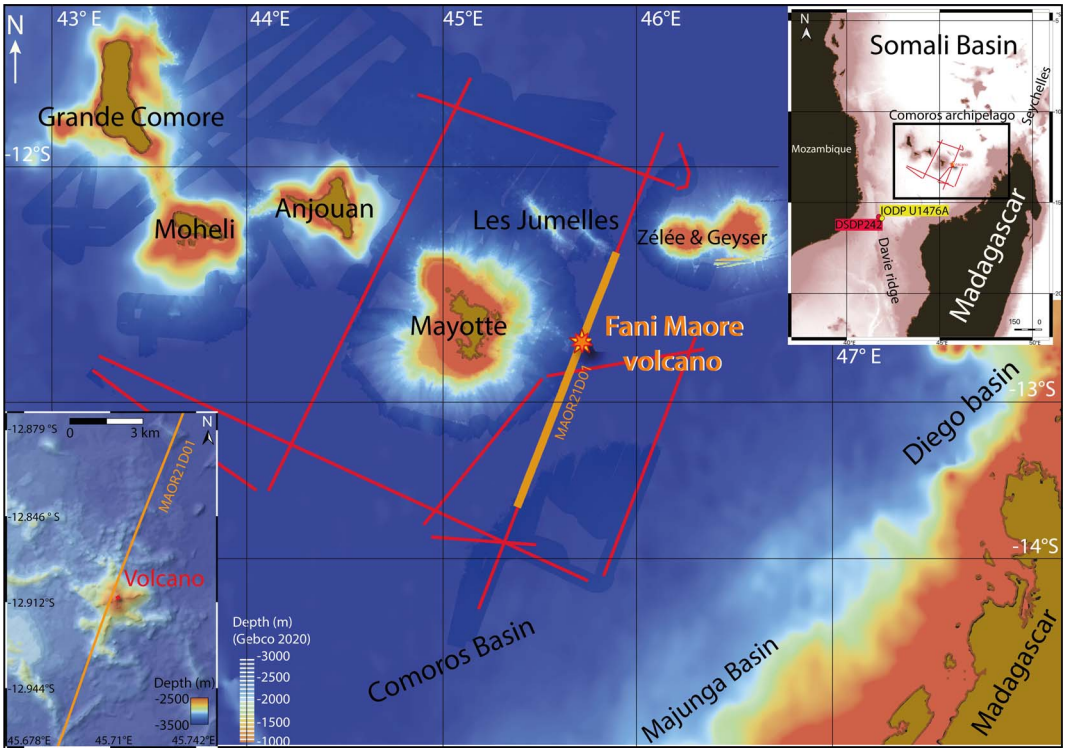

Figure 1. Location of the multichannel seismic profile MAOR21D01 (orange line) from SISMAORE MCS dataset (red lines) in the south of the Somali basin offshore the Comoros Archipelago, in the western Indian Ocean [see top-right inset; bathymetric data from Compilation Group GEBCO Grid, 2020]. Lower-left inset: bathymetric map of the Fani Maore volcano to the east of Mayotte [Thinon et al., 2020].

crust. We constrain the age of the onset of volcanic activity in the survey area by identifying a basaltic layer at depth that we relate to the early construction of Mayotte Island and correlating seismic horizons above and below, using known seismic stratigraphy.

2. Geological background

Volcanism in the northern Mozambique Channel is widespread since the Early Cretaceous [Sauter et al., 2018]. It initiated soon after the onset of seafloor spreading between Madagascar and Africa and continued as several phases until the present-day. In the West Somali Basin and the Mozambique Channel, the oldest regional magmatic phase occurred in Late Cretaceous times in relation to the breakup of Madagascar and Greater India [Torsvik et al., 2000]. Widespread flood basalts erupted between 92–83 Ma both onshore and offshore Madagascar [Leroux et al., 2020, Storey et al., 1995]. Renewed volcanic activity around the Mozambique Channel appeared to have started during Late Oligocene [Michon, 2016]. Based on geochronological data, the oldest volcanic activity recorded in the Comoros Archipelago has been dated around 11 Ma ago [Pelleter et al., 2014], but the timing of onset and main growth phase of the Archipelago remains poorly constrained [Michon, 2016]. Assuming an average long-term magma production rate for the Comoros Archipelago of 0.05 m^3/s, Michon [2016] suggested that volcanic activity initiated earlier in Mayotte, at about 20 Ma ago. The nature of the crust beneath the volcanic edifices remains a major open question. Both oceanic and extended continental crust have been proposed [Famin et al., 2020]. Using one receiver function, Dofal et al. [2021] recently proposed that the volcanic edifice of Mayotte Island was emplaced on top of an isolated continental block, abandoned during the Gondwana

break-up and thickened afterward by magmatic underplating. However, these data were compatible with both continental and oceanic crust, and the continental block model mainly relies on the presence of a quartzite massif, on Anjouan Island, which is west (i.e., oceanward) of Mayotte [Roach et al., 2017]. Thus, the nature of the crust under Mayotte is still subject to debate.

3. Data acquisition and processing

Multichannel seismic (MCS) data were recorded with a 6000 m long streamer with 960 channels spaced every 6.25 m and towed at 10 m depth. The streamer position was computed using a tail buoy GPS and compasses. The seismic reflection source was composed of 16 airguns in two clusters, with a total volume of ~82 L (4990 cu. in.), also towed at 10 m depth. The airgun array was triggered every 40 s, i.e., every 100 m with a mean vessel speed of 4.8 knots. The record length was 20 s with a sampling rate of 2 ms. The distance between each common depth point (CDP) is 3.25 m. During processing, supergather CDPs were built by merging 4 CDPs in a bin of 12.5 m, allowing for a fold of 60.

Processing followed a fairly typical workflow using Geovation® software (developed by CGG) in pre-stack time for almost all steps: trace editing, amplitude correction, normal move-out correction, FK-filtering, multiple attenuation and predictive deconvolution. Post-stack time migration was performed using velocity analysis. Velocities were manually picked every 200 CDP to update the velocity model (Figure 2 and Supplementary Figure 1). The first picking round resulted in a significant signal loss below ~5.25 s TWT (two-way travel time) after stacking (example around CDP 8001, Figure 2Aa, Ab and Ac, assuming a linear velocity increase with depth shown as red line in B). We iteratively improved the stack by increasing the RMS (root mean square) velocity at that depth (resulting interval velocities shown as black line in Figure 2B, improved stack in Ca, Supplementary Figure 1). The clearest reflectivity in the entire sedimentary column was obtained with a strong increase of the interval velocity followed by a velocity inversion defining a 4000 m/s layer between 5.25 s and 5.55 s TWT (at CDP 8001) (Supplementary Figure 2). Seismic reflectors beneath (Figure 2Ca, Cb and Cc) gain more coherency when the velocity inversion is included. Although we may sometimes miss the exact location of the velocity inversion due to the low resolution of velocity picking, a weak reflector marking the base of the layer can be followed consistently along most of the profile (Figure 3B, Ca, Cb). Below this layer, velocities must be back to levels expected for typical sedimentary layers (2000–3000 m/s; Figure 2A).

4. Description of the multichannel seismic reflection profile

The most striking shallow feature of the seismic reflection profile is the recent Fani Maore volcano, centered at CDP 12800 (distance ~99 km) (Figure 3A, B). The volcanic edifice is ~1 s TWT high and 10 km wide at its base. An important observation is that it sits on a series of subparallel reflectors, corresponding to a 0.12 s TWT thick sedimentary unit (quoted α in Figure 3B). Two smaller edifices, ~0.3 s TWT high and 1.3–1.8 km wide, are located on each side of the new volcano (centered at CDP 12400 and 13400). A strong reflector located below the volcanic edifices can be traced at ~4.75 s TWT all the way to the southern and northern ends of the profile, within the sedimentary unit (Figure 3A, B, C). This reflector corresponds to a strong velocity gradient at the top of the 4000 m/s interval velocity layer (see Section 3, Figure 2 and Supplementary Figure 2). Considering that this interval velocity is representative of typical basaltic rocks [Telford et al., 1990] and that the strong reflector at the top of the layer is below the volcanic edifices, we are confident that this reflector corresponds to the top of a basaltic unit. Sub-parallel reflectors, corresponding to sedimentary layers, are observed both above and below this volcanic layer (Figure 3). The entire sedimentary cover is thinner in the northernmost part of the profile (~2.5 s TWT thick converting to ~3.1 km using an average 2500 m/s velocity in the sediments) than at the southern end of the profile (3 s TWT, ~3.8 km) (Figure 3). The top basement is defined by a strong reflector at 7–8 s TWT below which continuous and fine layering is no longer observed, replaced by a series of discontinuous very low frequency phases.

4.1. *Seismic stratigraphy*

Calibration of MCS data in previous works [Franke et al., 2015, Klimke et al., 2016] is based on the stratig-

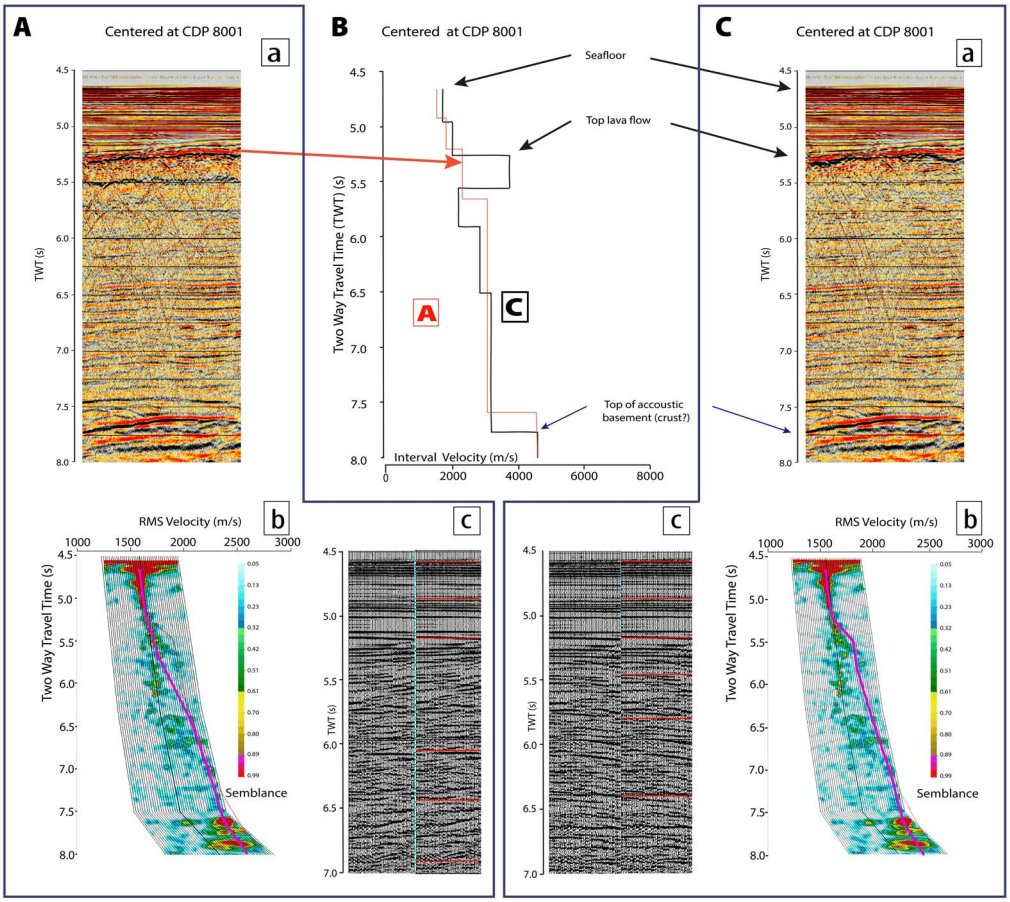

Figure 2. (A) Seismic processing using the velocity picking in red line (B) (a) Seismic image centered at CDP 8001 with the velocity model presented in (B) (red line); (b) RMS velocities (purple lines) as a function of TWT (s), shown on the semblance. These RMS velocities profiles have been applied to the stacked profile shown in (Aa); (c) Supergather 8001 after Normal Move Out correction (NMO) (red lines) corresponding to the stacked section (Aa). (B) Example of interval velocity of the supergather CDP 8001 as a function of the two-way travel time for two different velocity pickings (the red line corresponds to the RMS velocity picking shown in (Ab); the black line corresponds to the RMS velocity picking shown in (Cb)) (C) Seismic processing using the velocity picking in black line (B) (a) Seismic image centered around CDP 8001 after application of the full processing workflow with velocity inversion (B: black line), (b) RMS velocities (purple lines) as a function of TWT (s), shown on the semblance. These RMS velocities profiles have been applied to the stacked profile shown in Ca. (c) Stack section centered around CDP 8001 after NMO velocity picking, based on the first determination of velocities presented in Cb and B black line.

raphy obtained at DSDP (Deep Sea Drilling Project) hole 242 and IODP (Integrated Ocean Drilling Program) hole 1476, both located ~500 km west of Mayotte (inset in Figure 1), as well as ties with seismic lines of offshore Madagascar [Leroux et al., 2020]. Our revised seismic stratigraphy builds on these studies and the identification of four remarkable seismic markers in the sedimentary cover: top Miocene, top Oligocene, Cretaceous-Paleogene unconformity (K/Pg), and the Turonian volcanism event (Figures 3 and 4). Since they bracket the basaltic layer, they put strong constraints on the timing of Mayotte volcan-

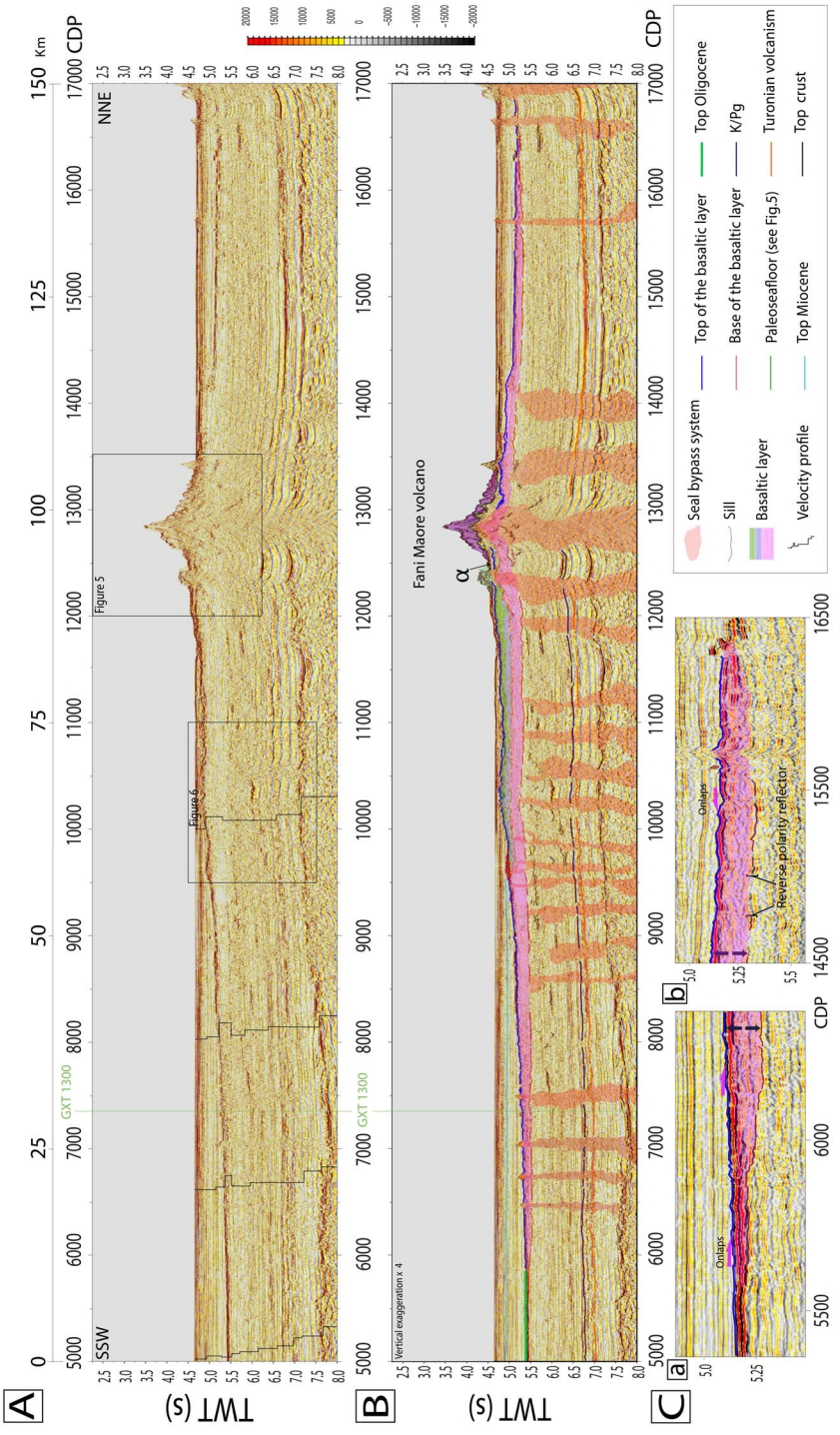

Figure 3. (A) Migrated profile MAOR21D01 with (B) interpretation from CDP 5000 to CDP 17000 (150 km, see Figure 1 for the location of the profile. The Fani Maore volcano is located at CDP 12900. (C) Termination of the basaltic layer on the southern (a) (vertical exaggeration ×4) and in the northern (b) (vertical exaggeration ×8) part of the line. Sediments are onlapping on its top.

ism. These markers are distinctively followed in the southern part of the profile but are more difficult to identify to the north of the new volcano.

The K/Pg unconformity is a distinct event recognized in the seismic profiles throughout the West Somali basin [Franke et al., 2015, Mahanjane, 2014]. Offshore northern Madagascar, this unconformity is well marked in the lines crossing the offshore Majunga Basin [Leroux et al., 2020]. One of these lines (ION GXT 1300) crosses our MAOR21D01 profile at CDP 7400 (Figure 3A, B, green vertical line) allowing us to correlate the medium amplitude reflector, more clearly visible at 6.75 s TWT at CDP 6000 (Figure 4), to the K/Pg unconformity (K/Pg blue line in Figures). A series of reflectors is onlapping the K/Pg unconformity at the southern end of the profile. Below the K/Pg reflector, we interpret a package of high amplitude and low-frequency discontinuous reflectors (TV in Figures 3 and 4, orange line) as corresponding to the Turonian volcanism that has been evidenced in the Diego and Majunga basins offshore Madagascar [Coffin and Rabinowitz, 1987, Leroux et al., 2020].

We identify a strong reflector as the top Oligocene horizon, based on the seismic stratigraphy used in Franke et al. [2015, TO in Figures 3 and 4] and the DSDP hole 242. This Oligocene horizon is well defined in the Rovuma basin [Mougenot et al., 1986] and can be followed from there up to the eastern flank of the Davie Ridge [Franke et al., 2015] and toward the Comoros Archipelago. Finally, we identify a top Miocene horizon (TM in Figures 3 and 4) at the same depth than the top-Miocene unit found in the IODP hole 1476 [235 m below sea floor, location in Figure 1; Hall et al., 2017].

4.2. *Description of the basaltic layer*

The top of the basaltic layer is a clear, strong reflector all along the MCS line (Figures 3A, B, and 4). To the south of the new volcano, this reflector gently dips ~1° southward, in continuity with the slope of the Mayotte edifice, measured from the bathymetric data in a sediment-free area. From the seismic image, it is clear that the sedimentary layers on top of the basaltic layer are progressively onlapping the top reflector on both sides of the Fani Maore volcano (Figure 3Ca). The top of the basaltic layer is highly reflective and smooth except where conic-shaped edifices are locally observed. Small conic-shaped edifices, ~500 m wide and ~200 m high, are most clearly imaged around CDP 7000 in the distal part of the volcanic layer (Figure 3). Another volcano around 4 km large and 150 m tall is observed at CDP 9600. To the north of this edifice, the top basaltic basement becomes rougher and irregular for ~20 km, before stepping upward and reaching the recent volcano area. A medium amplitude discontinuous flat reflector at ~5.7 s TWT is identified as the base of the basaltic layer. This reflector is characterized by his reverse polarity, more clearly visible on the northern part of the profile (see the red line in Figures 3Cb, 4, 5 and 6). This layer thins southward and ends as a single reflector at ~5.7 s TWT depth at the southernmost end of the MCS line (Figure 3).

In the southern part of the MCS line, three seismic facies are identified within the basaltic layer (pink, blue and green units to the south of the Fani Maore volcano in Figures 3–5). To the north, the facies of the basaltic layer appears more or less uniform (cyan layer to the north of the new volcano in Figures 3B and 5c). We interpret the deepest seismically transparent layer with a mean thickness of ~0.5 s TWT (~1000 m) as representing the main volcanic flow unit (see the pink layer in Figures 3B and 4c). It extends from CDP 5590 to CDP 12800 along ~91 km. Closer to the submarine volcano, a second basaltic unit overlays the bottom one, but still below the seismically distinct top reflection of the flow unit (blue layer in Figures 3B and 5c). This layer has a smaller extent (~33 km) and thickness (~0.25 s TWT, i.e., ~500 m on average) when compared to the main volcanic unit. The thickness of the upper part of the basaltic layer is highly variable and reaches 0.4 s TWT (800 m) close to the new volcanic edifice (see the green layer in Figures 3 and 5). To the north of the Fani Maore volcano, the basaltic layer extends from CDP 13500 to CDP 16500 (~35 km) and is made of a flat-lying unit (cyan layer in Figures 3B and 5c). A distinct step in the top reflector of this layer at CDP 14200 might represent a lava front. Close to the new volcano, the volcanic unit is ~0.3 s TWT thick (~700 m) while it thins to ~0.2 s TWT (~400 m) to the north of the step.

4.3. *The seal bypass systems*

Below the volcanic layer, numerous seal bypass systems [as defined by Cartwright et al., 2007] are ob-

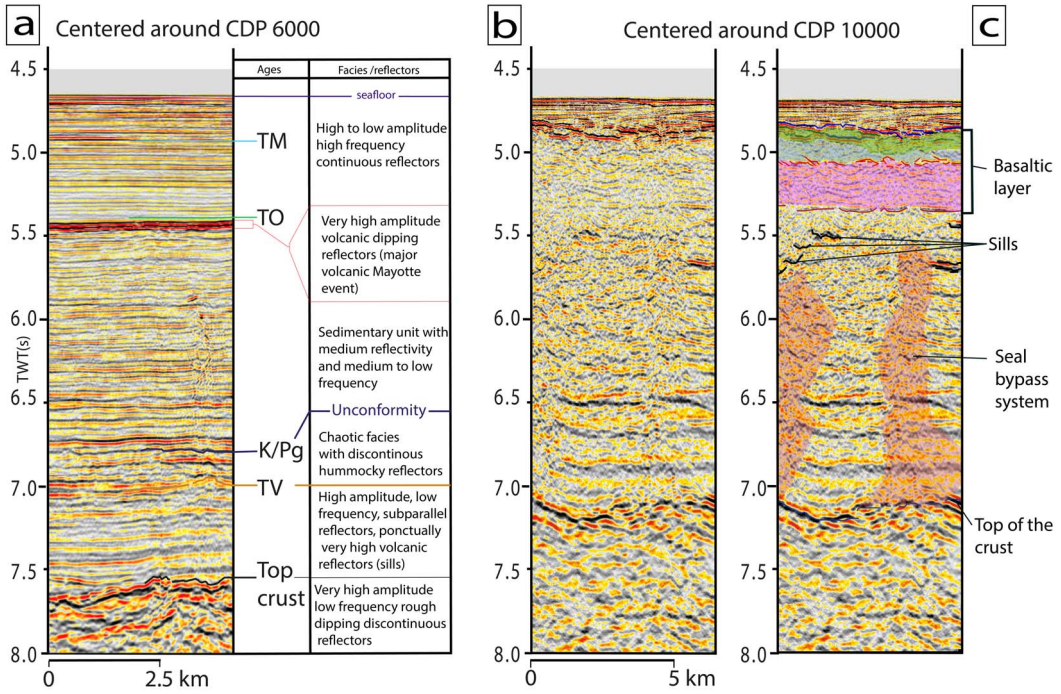

Figure 4. (a) Seismic stratigraphic horizons and associated facies identified at CDP 6000 (line MAOR21D01) TM: Top Miocene, TO: Top Oligocene, K/Pg: Cretaceous/Paleogene unconformity, TV: Turonian volcanism; (b, c) same profile at CDP 10000 and identification of seismic facies: basalt layer, sills, seal bypass system, and the top of the acoustic basement.

served (reddish domains in Figures 3–5). These seal bypass systems are recognized as chaotic chimney-like seismic facies running vertically through the sedimentary units. There, the typical continuous reflection pattern of the sedimentary units is replaced by scattered and strongly attenuated reflections. Locally, pull-up effects, due to vertical variations in velocity resulting from the occurrence of high-velocity magmatic material, disturb the geometry of the sedimentary units (as observed in TWT). Because there is often a progressive change of the seismic facies toward the centers of the seal bypass systems, defining precisely the edges of this seismic facies is difficult. The high-velocity basaltic layer above also acts as a screen filter and masks the imaging of the lower parts. Therefore, we only show the largest and best-defined seal bypass systems in Figures 3, 5 and 6. Such seal bypass systems are more numerous to the south of the new volcano while the chaotic seismic facies is more pervasive at a small scale in the northernmost part of the profile. There, beside smaller systems, we observe two seal bypass systems that cuts through the volcanic layer and the recent sedimentary layer rising up to the seafloor (Figure 3A, B; CDP 15700 and CDP 16600). At the end of the profile (CDP 17000) we observe some seal bypass system corresponding to the volcanic activity of the Jumelles ridges (Figure 1). All other seal bypass systems (without counting the seal bypass system present under the Fani Maore volcano) are sealed by the main volcanic layer. Seal bypass systems are narrow below small volcanic edifices and wider below the larger edifices, the largest one being observed beneath the new East-Mayotte volcano (Figure 5b, c). Numerous saucer-shaped bright reflectors, often organized step-wise, are observed both inside and at the border of the seal bypass systems. Although their shape might result from pull-up effects or migration artifacts (CDP 12700; at 5.0 s TWT), we interpret most of these bright amplitude reflectors as sills (Fig-

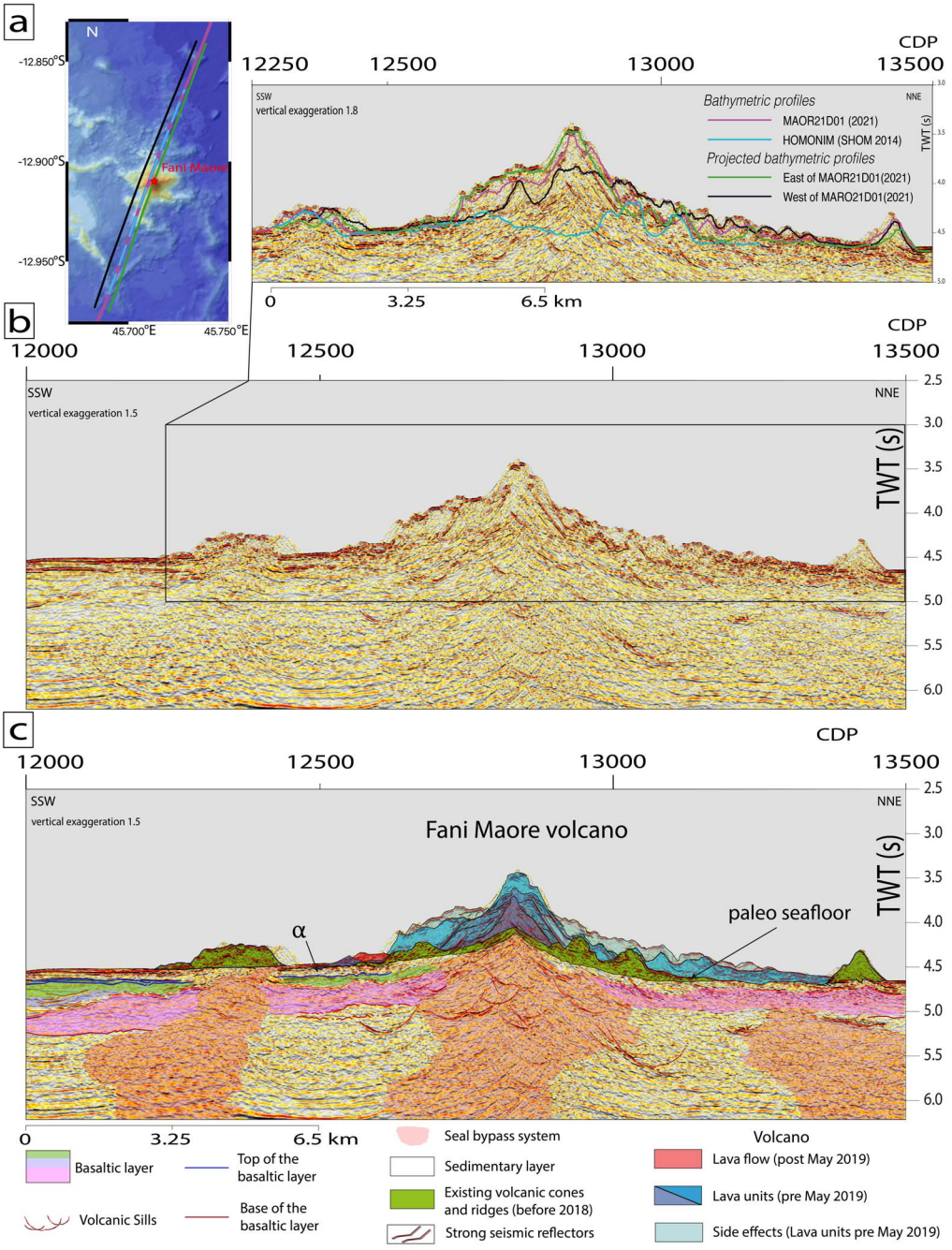

Figure 5. (a) Bathymetric profiles converted in s TWT plotted on the seismic profile MAOR21D01. Purple is from SISMAORE cruise [Thinon et al., 2020, 2022] dark blue from the HOMONIM project [SHOM, 2016a]. Parallel bathymetric profiles from SISMAORE cruise on either side of the seismic profile are projected onto the seismic profile. Seismic reflections above the purple line in the northern and southern parts of the volcano could be seismic side echoes from late flows on its flanks. (b, c) Close up view of the Fani Maore volcano from CDP 12000 to 13500 (18.75 km length, see Figure 3 for the location) and its interpretation. We identify the latest lava flows building the volcano since 2018 (in blue, purple and orange) and the paleo-seafloor (top of green surface); we define distinct facies into the basaltic layer (see Figure 6 for explanations).

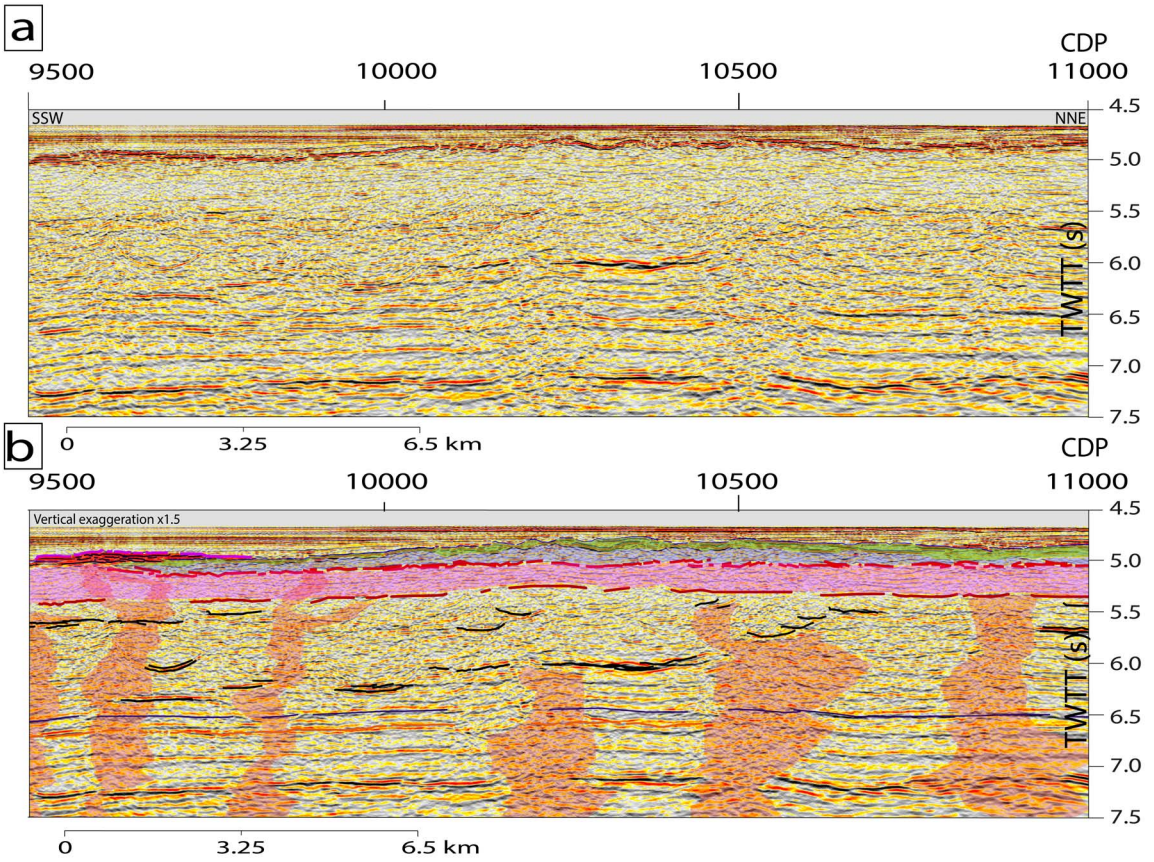

Figure 6. (a, b) Close-up view of the southern part of the MAOR21D01 profile from CDP 9500 to 11000 showing the seismic facies within the basaltic layer and below it within the seal bypass systems (see Figure 3 for the location).

ures 3A, B, 4, 6, and 7) [Medialdea et al., 2017]. We thus interpret the disturbed seismic facies in the seal bypass systems as the result of a network of almost vertical dykes or fractures, not imaged in seismic reflection, in which fluids and/or melt are rising from crustal or sub-crustal levels, up to the submarine volcanic edifices.

4.4. *The new volcanic edifice*

We use the bathymetric grid collected by the SHOM (Service hydrographique et océanographique de la marine) in 2014 [SHOM, 2016b, 2014] to obtain a time converted profile of the paleo-seafloor, using water interval velocity (the pull-up is not corrected). We superimpose this paleo-seafloor on the MCS profile (see the blue line in Figure 5a). This paleo-seafloor is not flat but shows some conic-shaped edifices that can be correlated with a strong undulating reflector in the MCS profile (see the green layer in Figures 3b and 5c). This reflector joins the seafloor at CDP 12500 to the south and CDP 13300 to the north defining the 10 km wide base of the new volcano (Figure 5b, c). To the north, the recent volcanic material abuts the adjacent smaller and older edifice (green in Figures 5, 7). To the south, the seafloor at the foot of the new volcano is flat if corrected for the pull-up effect from high-velocity material and at the same depth as the small older volcanic edifice to the south (CDP 12500 Figures 3, 5 and 7). This strongly argues for the presence of sediments at the seafloor there, rather than a magmatic flow unit. Indeed, between

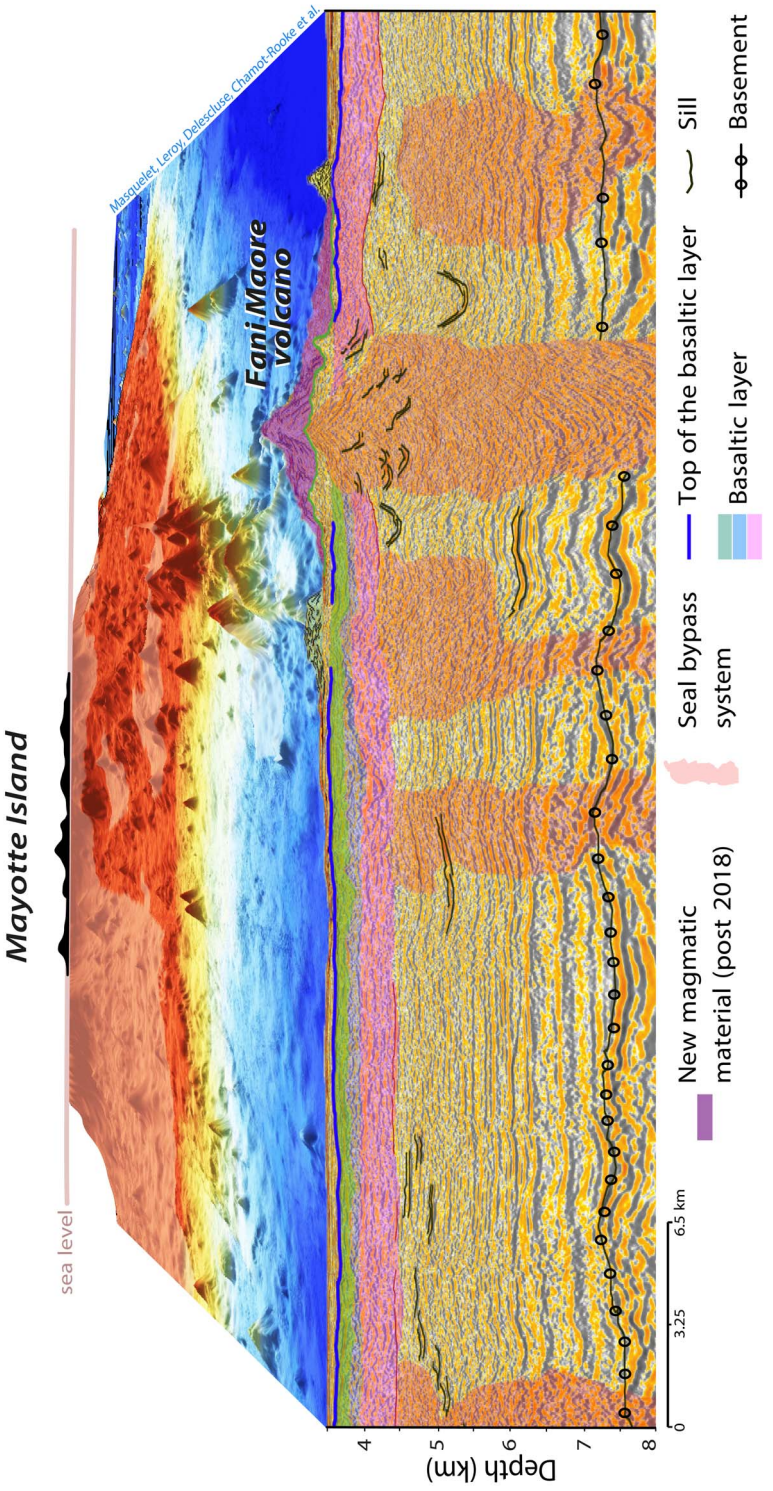

Figure 7. 3D close-up view of the Fani Maore volcano area with the interpreted seismic line MAOR21D01, converted in depth using our stack velocity model (see Supplementary material 1).

this paleo-seafloor and the main volcanic layers at depth (pink and cyan layers in Figures 3 and 5) we identify a ~0.11 s TWT (~140 m) thick unit which contains locally some fine reflectors that we propose to correspond to sedimentary layers. A few bright reflectors are also observed within this unit that could correspond to volcanic flows (α in Figures 3B and 5). Finally, under the Fani Maore volcano and below the basaltic layer, a series of subparallel reflectors corresponding to a sedimentary unit 1.75–2 s TWT thick (~2.2–2.5 km) is identified lying on the top of the acoustic basement (Figures 5 and 7). Numerous bright saucer-shaped reflectors (i.e., sills) are imaged both within and outside the large seal bypass system delineated below the new volcano.

Above the paleo-seafloor, i.e., within the Fani Maore volcano, we attempt to identify different seismic units based on their more or less transparent facies and specific geometries of reflectors (Figure 5c). Superimposing time corrected bathymetric profiles from either side of the seismic profile onto the seismic image (Figure 5a, black and green lines) shows that the southern and northern upper parts of the new volcanic edifice may correspond to seismic side echoes generated by late lava flows on the flanks (light blue areas in Figure 5c). The strongest reflectors, which are almost parallel to each other and are dipping away from the central and shallowest part of the volcano, are marking changes of seismic facies. Therefore, we interpret them as corresponding to the main lava flows at the end or start of the volcanic events building the successive volcanic cones (Figure 5c in purple and blue). Smaller and weaker reflectors within some of these seismic facies look similar to those found in lava deltas (see within the blue domain in darkest blue Figure 5c) indicating lateral progradation of the edifice flanks during the volcanic events. Thanks to a previous bathymetric survey in May 2019 [Feuillet et al., 2021] we could identify a single small post May 2019 lava flow in our profile (in orange in Figure 5).

5. Evolution of the volcanism

Parallel lava flows dipping away from the volcano's shallowest part indicate that they were likely fed by a single magma conduit. We propose that the new volcano was formed through successive eruptive events building stacked cones and associated flows. These lava flows covered the pre-existing conic-shaped edifices of the paleo seafloor. Following the results from Berthod et al. [2021b] and Berthod et al. [2022], the single small post May 2019 lava flow (in red in Figure 5) shows that most of Fani Maore edifice imaged by our seismic reflection profile was built between May 2018 and May 2019, correlated to the beginning of the seismic crisis. This lava flow and the underlying one appear to cover an about 140 m-thick sedimentary unit with minor volcanic additions in it (see α in Figure 5). Assuming a 3 cm/ky sedimentation rate, measured at IODP well 1476 [Hall et al., 2017], a ~4.6 Ma long period of tectonic quiescence with little volcanism, if any, is roughly estimated at this location.

The main magmatic phase that resulted in the formation of the deep basaltic units is obviously older. The distinct seismic facies of this main basaltic layer together with the numerous seal bypass systems feeding several volcanic edifices on top of it reveal a complex volcanic evolution around Mayotte Island with at least three volcanic phases. The thickest, deepest, and thus oldest, basaltic layer with its flat base parallel to the underlying sedimentary units, has the widest extent. Considering the location of the seismic line on the flank of Mayotte Island and the gentle slope of the basaltic layer inline with the one of the Mayotte edifice, it is likely that this volcanic layer corresponds to the submarine portion of the Mayotte Island volcanic edifice (Figures 3A, B, 6a, b, and 7). Following Leroux et al. [2020], we attribute this volcanic episode to the very early formation of Mayotte Island. The southern end of this volcanic layer lies below the inferred top-Oligocene seismic horizon (~23 Ma, Figures 3 and 4). Volcanism at Mayotte Island may thus have begun significantly earlier than previously thought [20 Ma, Michon, 2016]. We estimate the onset of this volcanism between 26 and 27 Ma ago by taking the 0.13 s TWT difference between the top-Oligocene horizon and the most distal part of the main volcanic layer (130 m at 2 km/s) and assuming a 30–35 m/Ma constant sedimentation rate during the Oligocene. We will reassess this age of the onset of volcanism at Mayotte and the nearby Comoros islands using the other MCS lines from the SISMAORE cruise in a forthcoming paper. We note that this age coincides with the beginning of the rift-related volcanism in the southern East African Rift System [26–25 Ma in the Rukwa Basin; Roberts

et al., 2012], as well as in Central Madagascar [28 Ma in the Ankaratra province, Bardintzeff et al., 2010]. Following Michon [2016] and Michon et al. [2022], this contemporary onset of volcanism suggests a genetic link at a regional scale.

6. Conclusions

The interpretation of a newly acquired multichannel seismic reflection profile across the new volcano in the east of Mayotte reveals that several distinct magmatic phases affected the area. The most recent phase resulted in the formation of the Fani Maore volcano through eruptive events building successive cones with associated flows since May 2018. The geometry of the lava flows around the submarine volcano suggests a melt supply through a single magma conduit. The new volcano sits on a ~140 m thick sedimentary layer, as inferred from the seismic reflection pattern, suggesting a period of volcanic quiescence. Beneath this sedimentary layer exists a major, volcanic layer up to ~1 km thick and extends as far as ~91 km to the south and ~33 km to the north of the recently formed submarine volcano. This unit is made up of several different seismic facies that may indicate successive volcanic phases. We interpret this major volcanic layer as being part of the early construction of the Mayotte volcanic edifice, with the presence of a complex magmatic feeder system below, being composed of many saucer-shaped sills and seal bypass systems. A ~2.2–2.5 km thick sedimentary unit is found between the main volcanic layer, below the new volcano, and the top of the crust. The identification of the top-Oligocene seismic horizon above the deepest tip of the main volcanic layer indicates that the onset of the volcanism at Mayotte Island may be older than previously thought.

Conflicts of interest

Authors have no conflict of interest to declare.

Acknowledgments

This paper is a contribution of COYOTES and SISMAORE teams (http://www.geocean.net/coyotes/doku.php?id=start). It benefited from the previous works of the REVOSIMA community. The processing and the detailed analysis of these geophysical and geological data are carried out mainly in the framework of the ANR COYOTES (ANR-19-CE31-0018, https://anr.fr/Projet-ANR-19-CE31-0018) project funded by the French ANR (Agence Nationale de Recherche) and the BRGM. The SISMAORE cruise was mainly funded by the Flotte Océanographique Française (FOF) and by the BRGM. We thank CGG for allowing us to use the CGG Geovation software in CNRS labs. We thank Captains P. Moimeaux and G. Ferrand, the crews and technicians from the R/V Pourquoi Pas? (FOF by IFREMER/GENAVIR). Thanks to the BRGM regional department of Mayotte. Thanks to REVOSIMA and DIRMOM for their assistance with the cruise during the COVID sanitary crisis. Masquelet's Ph.D. is funded by Sorbonne Université, via the ANR COYOTES.

Supplementary data

Supporting information for this article is available on the journal's website under https://doi.org/10.5802/crgeos.154 or from the author.

References

Bardintzeff, J.-M., Liégeois, J.-P., Bonin, B., Bellon, H., and Rasamimanana, G. (2010). Madagascar volcanic provinces linked to the Gondwana break-up: geochemical and isotopic evidences for contrasting mantle sources. *Gondwana Res.*, 18, 295–314.

Berthod, C., Komorowski, J.-C., Gurioli, L., Médard, E., Besson, P., Bachèlery, P., Verdurme, P., Chevrel, O., Di Muro, A., Devidal, J.-L., Nowak, S., Thinon, I., Burckel, P., Hidalgo, S., Deplus, C., Bermell, S., Réaud, Y., Fouchard, S., Bickert, M., Le Friant, A., Feuillet, N., Jorry, S., Fouquet, Y., Rinnert, E., Cathalot, C., and Lebas, E. (2022). Temporal evolution of the Mayotte eruption revealed by in situ submarine sampling and petrological monitoring. *C. R. Géosci.*, 354(S2). Online first.

Berthod, C., Médard, E., Bachèlery, P., Gurioli, L., Di Muro, A., Peltier, A., Komorowski, J.-C., Benbakkar, M., Devidal, J.-L., Langlade, J., Besson, P., Boudon, G., Rose-Koga, E., Deplus, C., Le Friant, A., Bickert, M., Nowak, S., Thinon, I., Burckel, P., Hidalgo, S., Kaliwoda, M., Jorry, S. J., Fouquet, Y., and Feuillet, N. (2021a). The 2018-ongoing Mayotte submarine eruption: magma migration imaged by

petrological monitoring. *Earth Planet. Sci. Lett.*, 571, article no. 117085.

Berthod, C., Médard, E., Di Muro, A., Hassen Ali, T., Gurioli, L., Chauvel, C., Komorowski, J.-C., Bachèlery, P., Peltier, A., Benbakkar, M., Devidal, J.-L., Besson, P., Le Friant, A., Deplus, C., Nowak, S., Thinon, I., Burckel, P., Hidalgo, S., Feuillet, N., Jorry, S., and Fouquet, Y. (2021b). Mantle xenolith-bearing phonolites and basanites feed the active volcanic ridge of Mayotte (Comoros archipelago, SW Indian Ocean). *Contrib. Mineral. Petrol.*, 176, article no. 75.

Cartwright, J., Huuse, M., and Aplin, A. (2007). Seal bypass systems. *Bulletin*, 91, 1141–1166.

Cesca, S., Letort, J., Razafindrakoto, H. N. T., Heimann, S., Rivalta, E., Isken, M. P., Nikkhoo, M., Passarelli, L., Petersen, G. M., Cotton, F., and Dahm, T. (2020). Drainage of a deep magma reservoir near Mayotte inferred from seismicity and deformation. *Nat. Geosci.*, 13, 87–93.

Coffin, M. F. and Rabinowitz, P. D. (1987). Reconstruction of Madagascar and Africa: evidence from the Davie Fracture Zone and western Somali Basin. *J. Geophys. Res.*, 92, article no. 9385.

Compilation Group GEBCO Grid (2020). Gridded Bathymetry Data.

Dofal, A., Fontaine, F. R., Michon, L., Barruol, G., and Tkalčić, H. (2021). Nature of the crust beneath the islands of the Mozambique Channel: constraints from receiver functions. *J. Afr. Earth Sci.*, 184, article no. 104379.

Famin, V., Michon, L., and Bourhane, A. (2020). The Comoros archipelago: a right-lateral transform boundary between the Somalia and Lwandle plates. *Tectonophysics*, 789, article no. 228539.

Feuillet, N., Jorry, S., Crawford, W. C., Deplus, C., Thinon, I., Jacques, E., Saurel, J. M., Lemoine, A., Paquet, F., Satriano, C., Aiken, C., Foix, O., Kowalski, P., Laurent, A., Rinnert, E., Cathalot, C., Donval, J.-P., Guyader, V., Gaillot, A., Scalabrin, C., Moreira, M., Peltier, A., Beauducel, F., Grandin, R., Ballu, V., Daniel, R., Pelleau, P., Gomez, J., Besançon, S., Geli, L., Bernard, P., Bachelery, P., Fouquet, Y., Bertil, D., Lemarchand, A., and Van der Woerd, J. (2021). Birth of a large volcanic edifice offshore Mayotte via lithosphere-scale dyke intrusion. *Nat. Geosci.*, 14, 787–795.

Franke, D., Jokat, W., Ladage, S., Stollhofen, H., Klimke, J., Lutz, R., Mahanjane, E. S., Ehrhardt, A., and Schreckenberger, B. (2015). The offshore East African Rift System: structural framework at the toe of a juvenile rift: THE OFFSHORE EAST AFRICAN RIFT. *Tectonics*, 34, 2086–2104.

Hall, I. R., Hemming, S. R., LeVay, L. J., and Scientists, E. (2017). South African climates (Agulhas LGM Density Profile). In *Proceedings of the International Ocean Discovery Program*, volume 361. International Ocean Discovery Program, College Station, TX.

Klimke, J., Franke, D., Gaedicke, C., Schreckenberger, B., Schnabel, M., Stollhofen, H., Rose, J., and Chaheire, M. (2016). How to identify oceanic crust—evidence for a complex break-up in the Mozambique Channel, off East Africa. *Tectonophysics*, 693, 436–452.

Lavayssière, A., Crawford, W. C., Saurel, J.-M., Satriano, C., Feuillet, N., Jacques, E., and Komorowski, J.-C. (2021). A new 1D velocity model and absolute locations image the Mayotte seismo-volcanic region. *J. Volcanol. Geotherm. Res.*, 421, article no. 107440.

Lemoine, A., Briole, P., Bertil, D., Roullé, A., Foumelis, M., Thinon, I., Raucoules, D., de Michele, M., Valty, P., and Hoste Colomer, R. (2020). The 2018–2019 seismo-volcanic crisis east of Mayotte, Comoros islands: seismicity and ground deformation markers of an exceptional submarine eruption. *Geophys. J. Int.*, 223, 22–44.

Leroux, E., Counts, J. W., Jorry, S. J., Jouet, G., Révillon, S., BouDagher-Fadel, M. K., Courgeon, S., Berthod, C., Ruffet, G., Bachèlery, P., and Grenard-Grand, E. (2020). Evolution of the Glorieuses seamount in the SW Indian Ocean and surrounding deep Somali Basin since the Cretaceous. *Mar. Geol.*, 427, article no. 106202.

Mahanjane, E. S. (2014). The Davie Fracture Zone and adjacent basins in the offshore Mozambique Margin—a new insights for the hydrocarbon potential. *Mar. Pet. Geol.*, 57, 561–571.

Medialdea, T., Somoza, L., González, F. J., Vázquez, J. T., de Ignacio, C., Sumino, H., Sánchez-Guillamón, O., Orihashi, Y., León, R., and Palomino, D. (2017). Evidence of a modern deep water magmatic hydrothermal system in the Canary Basin (eastern central Atlantic Ocean). *Geochem. Geophys. Geosyst.*, 18, 3138–3164.

Michon, L. (2016). The volcanism of the Comoros Archipelago integrated at a regional scale. In

Bachelery, P., Lenat, J.-F., Di Muro, A., and Michon, L., editors, *Active Volcanoes of the Southwest Indian Ocean, Active Volcanoes of the World*, pages 333–344. Springer, Berlin, Heidelberg.

Michon, L., Famin, V., and Quidelleur, X. (2022). Evolution of the East African Rift System from trap-scale to plate-scale rifting. *Earth-Sci. Rev.*, 231, article no. 104089.

Mougenot, D., Recq, M., Virlogeux, P., and Lepvrier, C. (1986). Seaward extension of the East African Rift. *Nature*, 321, 599–603.

Pelleter, A.-A., Caroff, M., Cordier, C., Bachelery, P., Nehlig, P., Debeuf, D., and Arnaud, N. (2014). Melilite-bearing lavas in Mayotte (France): an insight into the mantle source below the Comores. *Lithos*, 208–209, 281–297.

Rinnert, E., Feuillet, N., Fouquet, Y., Jorry, S., Thinon, I., and Lebas, E. (2019). MAYOBS Cruises.

Roach, P., Milsom, J., Toland, C., Matchette-Downes, C., Budden, C., and Riaroh, D. (2017). New evidence supports presence of continental crust beneath the Comoros. In *Proceedings of the PESGB/HGS Africa Conference*, volume 18.

Roberts, E. M., Stevens, N. J., O'Connor, P. M., Dirks, P. H. G. M., Gottfried, M. D., Clyde, W. C., Armstrong, R. A., Kemp, A. I. S., and Hemming, S. (2012). Initiation of the western branch of the East African Rift coeval with the eastern branch. *Nat. Geosci.*, 5, 289–294.

Sauter, D., Ringenbach, J. C., Cannat, M., Maurin, T., Manatschal, G., and McDermott, K. G. (2018). Intraplate deformation of oceanic crust in the West Somali Basin: insights from long-offset reflection seismic data. *Tectonics*, 37, 588–603.

SHOM (2014). Transit valorisé de Mayotte à Brest.

SHOM (2016a). Homonin Project.

SHOM (2016b). MNT Bathymétrique de la Façade de Mayotte.

Storey, M., Mahoney, J. J., Saunders, A. D., Duncan, R. A., Kelley, S. P., and Coffin, M. F. (1995). Timing of hot spot—related volcanism and the breakup of Madagascar and India. *Science*, 267, 852–855.

Telford, W. M., Geldart, L. P., and Shériff, R. E. (1990). *Applied Geophysics*. Cambridge University Press, New York.

Thinon, I., Lemoine, A., Leroy, S., Paquet, F., Berthod, C., Zaragosi, S., Famin, V., Feuillet, N., Boymond, P., Masquelet, C., Mercury, N., Rusquet, A., Scalabrin, C., Van der Woerd, J., Bernard, J., Bignon, J., Clouard, V., Doubre, C., Jacques, E., Jorry, S., Rolandone, F., Chamot-Rooke, N., Delescluse, M., Franke, D., Watremez, L., Bachèlery, P., Michon, L., Sauter, D., Bujan, S., Canva, A., Dassie, E., Roche, V., Ali, S., Sitti Allaouia, A. H., Deplus, C., Rad, S., and Sadeski, L. (2022). Volcanism and tectonics unveiled in the Comoros archipelago between Africa and Madagascar. *C. R. Géosci.*, 354(S2). Forthcoming.

Thinon, I., Leroy, S., and Lemoine, A. (2020). SISMAORE cruise, RV Pourquoi pas ?

Torsvik, T. H., Tucker, R. D., Ashwal, L. D., Carter, L. M., Jamtveit, B., Vidyadharan, K. T., and Venkataramana, P. (2000). Late Cretaceous India-Madagascar fit and timing of break-up related magmatism. *Terra Nova*, 12, 220–224.